ARTICLE

OBC
www.rsc.org/obc

Mechanism and structure–reactivity relationships for aromatic hydroxylation by cytochrome P450

Christine M. Bathelt,[a] Lars Ridder,[b] Adrian J. Mulholland*[a] and Jeremy N. Harvey*[a]

[a] *School of Chemistry and Centre for Computational Chemistry, University of Bristol, Cantock's Close, Bristol, UK BS8 1TS. E-mail: jeremy.harvey@bris.ac.uk; Fax: +44 117 925 1295; Tel: +44 117 954 6991*

[b] *Molecular Design and Informatics, N.V. Organon, P.O. Box 20, 5340 BH Oss, The Netherlands*

Received 16th July 2004, Accepted 1st September 2004
First published as an Advance Article on the web 28th September 2004

Cytochrome P450 enzymes play a central role in drug metabolism, and models of their mechanism could contribute significantly to pharmaceutical research and development of new drugs. The mechanism of cytochrome P450 mediated hydroxylation of aromatics and the effects of substituents on reactivity have been investigated using B3LYP density functional theory computations in a realistic porphyrin model system. Two different orientations of substrate approach for addition of Compound I to benzene, and also possible subsequent rearrangement pathways have been explored. The rate-limiting Compound I addition to an aromatic carbon atom proceeds on the doublet potential energy surface *via* a transition state with mixed radical and cationic character. Subsequent formation of epoxide, ketone and phenol products is shown to occur with low barriers, especially starting from a cation-like rather than a radical-like tetrahedral adduct of Compound I with benzene. Effects of ring substituents were explored by calculating the activation barriers for Compound I addition in the *meta* and *para*-position for a range of monosubstituted benzenes and for more complex polysubstituted benzenes. Two structure–reactivity relationships including 8 and 10 different substituted benzenes have been determined using (i) experimentally derived Hammett σ-constants and (ii) a theoretical scale based on bond dissociation energies of hydroxyl adducts of the substrates, respectively. In both cases a dual-parameter approach that employs a combination of radical and cationic electronic descriptors gave good relationships with correlation coefficients R^2 of 0.96 and 0.82, respectively. These relationships can be extended to predict the reactivity of other substituted aromatics, and thus can potentially be used in predictive drug metabolism models.

Introduction

The cytochromes P450 are a ubiquitous family of haemproteins, which are capable of a variety of oxidation reactions. These enzymes are involved in a number of vital processes, such as biosynthesis, degradation of xenobiotics, carcinogenesis and drug metabolism. In the latter area, a particularly important reaction[1,2] is hydroxylation of C–H bonds, which can influence the bioavailability of pharmaceuticals, transform a pro-drug to its active form, or equally produce toxic metabolites. A detailed understanding of the mechanism of the reactions is vital for predicting conversions of pharmaceuticals and other xenobiotics, and hence for drug development. The rate and selectivity of cytochrome P450 substrate oxidation is co-determined by steric effects[3] in the enzyme active site and intrinsic electronic reactivity.[4] Depending on the substrate and the specific cytochrome P450, the selection of substrates and hydroxylation sites can be dominated by either orientation effects in the binding site or chemical reactivity of the various positions of the substrates. Here we address the intrinsic electronic contribution to selectivity and reactivity in arene oxidation, which has not been widely studied to date.

The reaction cycle of cytochrome P450 is complicated, involving a number of individual steps, each of which can be rate-limiting depending on the specific reaction and enzyme. This means the actual oxidation step is not always rate-limiting in the overall catalytic cycle of cytochrome P450 enzymes.[1,5] However, if alternative products can be formed from a given substrate, differences in reactivity will be observed. Thus, structure–reactivity relationships for the oxidation step can be valuable for predicting regioselectivity of substrates.

The putative catalytically active species involved in hydroxylation is assumed to be an oxoiron(IV) porphyrin radical cation, called Compound I,[6,7] in analogy to the corresponding chloroperoxidase (CPO) Compound I species. Cytochrome P450 Compound I has not been detected unambiguously due to its high reactivity, although there is indirect evidence for its existence.[8,9] Experimental observations[10–12] on CPO-Compound I suggest that it has a doublet ground state with two parallel unpaired electrons on the iron-oxo moiety and an antiparallel electron in a π-orbital of the porphyrin ligand. Theoretical studies[13–20] predict that the ground state of Compound I in the protein is a quasi-degenerate pair of triradicaloid states, labelled $^2A_{2u}$ and $^4A_{2u}$. They only differ in the spin coupling between the electronic triplet on the iron-oxo moiety and an electron in the a_{2u}-like (π) orbital of the porphyrin ring.

Hydroxylation of aliphatic substrates by Compound I is believed to proceed *via* the "hydrogen abstraction/oxygen rebound" mechanism,[21] which is supported by intrinsic kinetic isotope effect measurements[22,23] and observations of stereochemical scrambling.[24,25] In this pathway Compound I abstracts a hydrogen from the substrate to give a radical intermediate, which then recombines with the iron hydroxide species. Recently controversies arose due to radical-clock experiments,[26–29] which showed unrealistically short lifetimes of the intermediate radicals and rearrangement patterns corresponding to carbocationic species. Thus, an alternative "two-oxidant mechanism"[26–32] has been proposed involving the iron hydroperoxo species (Compound 0), as a second oxidant. Mutagenesis studies suggested that, when formation of Compound I is suppressed, sulfoxidation[30] and epoxidation[31,32] can be accomplished by Compound 0. However, recent density functional theory (DFT) calculations[33,34] show that Compound 0 is not reactive enough to serve as a second electrophilic oxidant with less active substrates. Instead, theoretical studies on alkane[35–43] and alkene[44–46] hydroxylation proposed a two-state-reactivity of Compound I as the sole oxidant involving both doublet and quartet A_{2u} states. On

DOI: 10.1039/b410729b

the low spin surface the reaction was shown to proceed *via* a barrierless recombination and thus is effectively an insertion, while the reaction on the high spin surface has a considerable barrier to recombination and thus gives true radical intermediates. DFT also suggests that electron transfer can occur in the initially formed radical pair to yield carbocations, thereby explaining the formation of characteristic rearranged products and of dehydrogenated products (obtained from deprotonation of the cations).[43,47]

Aromatic hydroxylation has been studied less extensively. Early studies[48,49] concluded that arene epoxides are obligatory intermediates in aromatic hydroxylation, mainly due to the observed NIH-shift,[50,51] the migration of hydrogen from the site of hydroxylation to the adjacent carbon. More recently experimental evidence[52,53] appeared for an alternative mechanism, which does not proceed *via* an epoxide intermediate. In this pathway Compound I adds to a substrate carbon forming a tetrahedral intermediate σ-complex, which can be radical-like or carbocation-like. All further products, phenol, ketone and epoxide, are generated by rearrangement of these σ-complexes. This is supported by theoretical investigations[54–56] ruling out a concerted epoxidation as an initial step in aromatic hydroxylation. Recent DFT computations[56] showed that in contrast to aliphatic hydroxylation, benzene hydroxylation only occurs on the low-spin surface and proceeds predominantly through an electrophilic pathway *via* a cation-like σ-complex intermediate. It was also found that the rearrangement of the cationic intermediate to phenol and ketone can be catalyzed directly by the enzyme through the N-protonated porphyrin intermediate, which serves as a proton shuttle.

Based on these previous findings on benzene hydroxylation it is desirable to extend these investigations to substituted aromatics, as an understanding of how substituents affect the ease of substrate oxidation should help in predicting human drug metabolism.

It has been shown that computational studies can perform well in describing trends within a series of related molecules.[57,58] In the absence of systematic experimental data, calculations using a reliable level of electronic structure theory can give valuable insight into substrate reactivity.

Earlier theoretical investigations of substituent effects in aromatic hydroxylation were based on computations at the AM1 semiempirical level using a simplified Compound I model or considering frontier orbital characteristics of the substrate alone. Rietjens *et al.*[53] predicted experimentally observed regioselectivities in fluorobenzenes by calculating the density distribution of the π-electrons over the different hydroxylation sites in the substrates. They also showed that the experimental rates of *p*-hydroxylation of a series of halogenated anilines correlate with the energy of the reactive HOMO electrons of the compounds.[5] This correlation suggests that reactivity in aromatic hydroxylation depends fully on the nucleophilic reactivity of the substrates. The range of substrates in this study, however, is restricted to halogens and it remains to be established if the effect of nucleophilicity is equally dominant over a wider range of substrates. A wider range of substituents in benzene hydroxylation was considered in a study by Jones *et al.*[59] The methoxy radical was used by these authors as a model for Compound I, but this does not represent the Compound I systems accurately because the porphyrin ring and the iron-oxo group participate in the electron transfer between the substrate and Compound I.

Density functional theory can provide models that are more accurate and reliable than those derived from calculations at the semi-empirical level. The B3LYP functional has been found to give accurate results and to make high-quality predictions of energetics in bioinorganic systems, such as P450 Compound I[13–20] and other transition metal complexes.[60–62] Following our preliminary study,[63] we use density functional theory and a full haem model to calculate activation energies for various substituted benzenes. Correlations of these values with experimentally and quantum chemically derived molecular descriptors have been tested to develop a new predictive model for the intrinsic reactivity. Here, we present a simple structure–reactivity relationship based on a range of very different substituents on benzene. The large, realistic model used in our calculations combined with the higher level of theory is likely to give more accurate results than previous studies on substituted aromatics. Our calculations reveal that the transition state in aromatic addition has considerable radical character, thus nucleophilic reactivity is not likely to fully explain tendencies in substrate hydroxylation. It is shown that both radical and cationic descriptors of substituents need to be taken into account to predict the trends in reactivity for aromatic hydroxylation in cytochromes P450.

Computational details

The model system we use is shown in Fig. 1; it consists of the iron, all groups coordinating to the iron, and the substrate molecule. The porphyrin is devoid of side chains and the cysteinato group is described by a methyl mercaptide group. Shaik *et al.*[18,40] found that the more simple HS^- ligand is in some respects a better mimic for the full cysteinato ligand as it leads to a similar ordering of electronic states. However CH_3S^- is sterically more realistic and resembles the cysteinato group in terms of ionization potential as found in other studies.[15,35,36,41] Calculations were carried out with the Jaguar 4.0 and 5.0 software[64] using the unrestricted hybrid density functional UB3LYP. Geometry optimizations were performed using the standard Los Alamos effective core potential and the associated triple-zeta contraction of the LACVP[65] basis, as implemented in Jaguar, on Fe (LACV3P basis), and the 6-31G* basis on all other atoms (BSI). In some cases, single point calculations at optimized geometries were performed with the same LACV3P basis on Fe, but the larger 6-311+G** basis on the other atoms (BSII). These B3LYP/BSII//B3LYP/BSI energies are very similar to the B3LYP/BSI energies. As found in previous studies[13–20] Compound I has several close-lying electronic states, and care must be taken to obtain the correct orbital occupation. Compound I was optimized with C_s symmetry constraints to avoid mixing of different electronic states. Geometries of intermediate and product complexes were optimized without symmetry constraints, although the optimized geometries were close to being C_s symmetry. Transition states for addition of Compound I to benzene and substituted benzenes were obtained in a two-step procedure. First, an energy profile was generated by optimizing the geometry at a large number of fixed O–C distances between the aromatic carbon atom and the oxygen atom of Compound I. Then full TS geometry optimization was carried out. Frequency analysis of the transition states for benzene, to verify their character, was performed with Gaussian98[66] using the same basis set as for calculations in Jaguar. Electronic effects of the protein were taken into account approximately by computing single point energies using an electrostatic continuum model, as implemented in Jaguar, with the dielectric constant set to 4.0. The cavity in the dielectric medium was generated using standard van der Waals radii and a solvent probe radius of 2.6 Å.

Geometries for the hydroxy adducts of substituted benzenes in the development of a quantitative structure activity relationship were optimized using the 6-31G(d) basis set, and single point energies were calculated using the 6-311+G(d,p) basis set.

Results and discussion

Benzene hydroxylation

We first addressed the addition of Compound I to benzene. We investigated two pathways, which differ in the orientation of the approach of benzene, but otherwise proceed through very similar

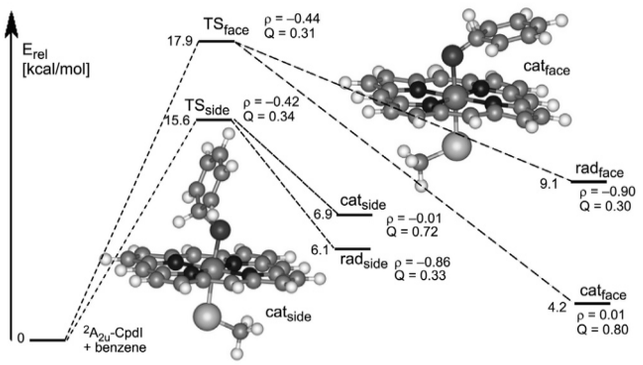

Fig. 1 B3LYP/BSII//B3LYP/BSI potential energy surfaces for face-on and side-on addition of benzene to the Compound I model species, including energies for both cation-like (cat) and radical-like (rad) adducts. Also shown are charges (Q) and spin (ρ) densities on the benzene moiety as derived from NBO analysis, and optimised structures of the cation-like adducts for both modes of approach.

electronic states. In one pathway benzene was approached with the plane of the benzene ring parallel to (face-on) the porphyrin plane, and in the other pathway the plane of the benzene ring was perpendicular to (side-on) the porphyrin plane (Fig. 1).

1. Face-on approach of benzene. In previous work,[54,55,67] Compound I addition to aromatics has been considered to proceed with a face-on approach of the ring towards the oxo group, and we too initially considered this mode of reaction. The lowest energy pathway was found to be an electrophilic addition leading from the $^2A_{2u}$ ground state of Compound I to a purely cationic intermediate. During this addition, two electrons of the substrate are transferred into singly occupied orbitals of Compound I, the porphyrin a_{2u} orbital and the π_{xz}* orbital on the FeO moiety. NBO charge and spin analysis of the corresponding transition state $\mathbf{TS_{face}}$ demonstrated that the electronic structure of the transition state is of a mixed cationic and radical nature, with considerable spin and charge transferred to the substrate (Fig. 1). As shown in Fig. 1, the spin density ρ on the ring is negative, which corresponds to an excess of β spin density in the benzene orbital involved in the electron transfer from benzene to Compound I. At certain points along the reaction coordinate the wavefunction could be converged to two different electronic states lying close in energy, one with more radical-like character and one with more cation-like character. In the fully optimized adducts the cation-like state drops below the radical-like state and is more favorable by 4.9 kcal mol^{-1} (Fig. 1). Attempts to localize a second transition state failed as higher lying electronic states dropped to the lower transition state TS_{face} discussed above. Alternative energy pathways for the quartet spin multiplicity were also considered by carrying out potential energy scans. Profiles starting from the $^4A_{2u}$ state of Compound I led to Compound I–benzene adducts in two different quartet states with transition states that were higher lying than the transition state for the doublet electrophilic pathway (calculations performed with basis set BSI showed that the lowest transition state for the quartet pathway was 3 kcal mol^{-1} above the doublet transition state TS_{face}).

Frequency analysis of the lowest energy electrophilic transition state TS_{face} with Jaguar was problematic as numerical round-off errors led to inaccuracies in the magnitude of the low-frequency modes. Upon calculating the frequencies with Gaussian98, one large imaginary frequency (452.3i cm^{-1}) was obtained, whose corresponding eigenvector clearly corresponds to the reaction coordinate. However, one additional small imaginary frequency (31.7i cm^{-1}) was also obtained. This suggests that the face-on transition state corresponds to a higher order saddle point rather than a true transition state. However the additional imaginary frequency is very small, and it is possible that in some of the substituted cases, or indeed in the protein, such a mode of approach does indeed correspond to a true transition state.

Table 1 Gas-phase and solution energy (B3LYP/BSI in kcal mol^{-1}) of the cation-like tetrahedral adduct relative to the radical-like one

	E_{rel} (gas-phase)	E_{rel} (ε = 4)
CN	—[a]	
Cl	+1.7	−0.5
H	+1.3	−1.5
F	+0.3	−3.2
CH_3	−0.1	−3.8
Nacetyl	−3.6	−8.0
OMe	—[b]	

[a] Only the radical-like state could be calculated. [b] Only the cation-like state could be calculated.

2. Side-on approach of benzene. In the case of the side-on approach of benzene to Compound I, a transition state ($\mathbf{TS_{side}}$) was located which shows spin and charge densities on benzene similar to those at the face-on electrophilic transition state, but lies 2.3 kcal mol^{-1} lower in energy (Fig. 1). This transition state corresponds to a true saddle point as confirmed by a single imaginary frequency (378.9i cm^{-1}).

On the product side, calculations carried out in the gas-phase indicate that the radical-like state of the tetrahedral intermediate lies slightly (0.8 kcal mol^{-1}) lower in energy than the cation-like one. This ordering is in contrast to the face-on benzene approach, where the cation-like state is more stable. This might be due to the better interaction of the positive charge on the benzene ring with the negative charge on the porphyrin ring in the face-on orientation. However, when using a solvent continuum model to describe at least roughly the enzyme environment, the cation-like intermediate is predicted to be the more stable (by 1.5 kcal mol^{-1}) also in this case (see H in Table 1). This suggests that in the polarizing environment of a protein, hydroxylation of benzene proceeds *via* a cation-like intermediate rather than a radical-like one.

Rearrangement pathways

We considered further reactivity by locating transition states for rearrangement of the cation-like tetrahedral adducts $\mathbf{cat_{face}}$ and $\mathbf{cat_{side}}$ (Fig. 1) to a complex of the ferric P450 system with either benzene epoxide or the ketone tautomer of phenol (the "NIH shift"[50,51] product, $\mathbf{ket_{face}}$, $\mathbf{ket_{side}}$ in Fig. 2). Note that all energies for the rearrangement pathways presented here were calculated at the B3LYP/BSI level. However, single point energies (B3LYP/BSII//B3LYP/BSI) computed for some of the species gave very similar results.

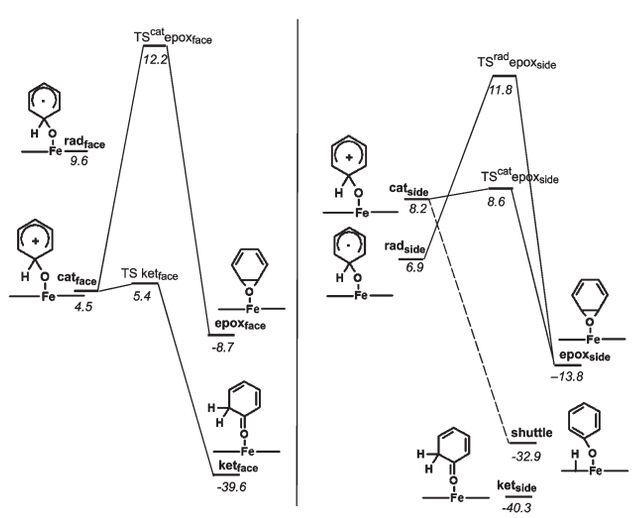

Fig. 2 Rearrangement pathways for the tetrahedral adducts fromed from the face-on (left) and side-on (right) addition to benzene. Relative energies (B3LYP/BSI) in kcal mol^{-1}.

1. Face-on benzene adduct. The epoxide and ketone species lie respectively at −8.7 and −39.6 kcal mol^{-1} relative to the reactants. The barrier for epoxide formation lies 7.7 kcal mol^{-1} above the cationic adduct, or, in other words, 12.2 kcal mol^{-1} above the reactants, and 6.9 kcal mol^{-1} lower than the TS for the initial addition step. During this transformation the C–C–O angle goes from 118° in the cationic adduct to 94° in the transition state to 58° in the product, and a gradual forming of the O–C bond is observed, with the O–C distance going from 2.4 Å to 2.1 Å in the transition state to 1.4 Å in the epoxide product.

For ketone formation *via* a 1,2 hydride shift a very small barrier of 0.9 kcal mol^{-1} was found by full transition state optimization at the lower level of theory (BSI). This barrier disappeared completely upon single point energy calculation (BSII) at the optimized geometry, with the TS computed to lie 2.4 kcal mol^{-1} below the cationic adduct. The distance between the migrating H atom and the *ortho*-carbon atom on benzene decreased from 2.0 Å in the cationic adduct to 1.7 Å in the transition state to a C–H bond length of 1.1 Å in the ketone complex.

2. Side-on benzene adduct. A very low barrier of 0.4 kcal mol^{-1} was found for rearrangement of the cation-like adduct to the epoxide. Relative to the reactants this corresponds to a barrier height of 8.6 kcal mol^{-1}, which is considerably lower than the barrier for initial formation of the tetrahedral adducts from Compound I. The O–C–C angle in the tetrahedral adduct (**cat$_{side}$** in Fig. 1) is less wide (109°) than in the face-on pathway (118°) and thus provides a better starting geometry for epoxide formation. In the transition state this angle decreases to 101° and ends in a 59° angle in the epoxide product. As in the face-on pathway the O–C distance, corresponding to the forming bond, decreases gradually, from 2.4 Å in the cationic adduct to 2.2 Å at the transition state to 1.5 Å in the epoxide. As cation-like and radical-like tetrahedral adducts lie relatively close in energy in the side-on pathway, we also located the transition state for rearrangement from the radical-like adduct (**rad$_{side}$** in Fig. 2) to the epoxide product. For this process a considerably higher barrier of 4.9 kcal mol^{-1} was calculated. In contrast to the face-on approach of benzene, a transition state for direct rearrangement to the ketone product (**ket$_{side}$** in Fig. 2) could not be located in the side-on pathway. Upon attempts to optimize such a TS, an N-protonated porphyrin complex (shuttle in Fig. 2) was formed instead, in which the *ipso*-hydrogen from the cationic adduct is transferred to one of the nitrogen atoms of the porphyrin ring. This is consistent with a previous study,[56] which found a very low barrier to this proton transfer, and proposed a proton-shuttle mechanism for formation of ketone and phenol *via* the N-protonated intermediate. The low activation barriers for both epoxide formation and formation of the N-protonated species from the cation-like adduct **cat$_{side}$** in the side-on pathway suggest that the reaction pathway *via* a cation-like rather than a radical-like adduct is favoured due to rapid subsequent product formation. In the face-on orientation of the tetrahedral adduct **cat$_{face}$** the hydrogen atom faces away from the porphyrin plane (Fig. 1) and can therefore not be abstracted by a porphyrin nitrogen to form the proton shuttle species. However, as discussed above, direct rearrangements of the cation-like adduct to epoxide and ketone complexes (**epox$_{face}$** and **ket$_{face}$** in Fig. 2) are possible and show low barriers.

While for the face-on approach direct rearrangement to the ketone is more favourable than epoxide formation, for the side-on approach, formation of the epoxide, both by direct rearrangement and *via* the shuttle species, is competitive with ketone formation.

In both side-on and face-on pathways the first step in benzene hydroxylation has a considerable barrier, while all subsequent rearrangements have low barriers. Hence, addition of Compound I to substrate is the most important reaction step in determining the reactivity of substrates, and we therefore focus on this process in the following investigations.

Table 2 Computed (B3LYP/BSI NBO analysis) charge (Q) and spin (ρ) densities for side-on addition TSs to *para*-substituted benzenes

	Q	Q (ε = 4)	ρ	ρ (ε = 4)
H	0.33	0.37	−0.43	−0.47
NO_2	0.17	0.18	−0.31	−0.39
NMe_2	0.44	0.55	−0.41	−0.49
OMe	0.37	0.41	−0.37	−0.40
Cl	0.31	0.33	−0.41	−0.42

Substituent effects on benzene hydroxylation

To understand the intrinsic electronic effects on reactivity in arene oxidation, we studied the barrier heights for addition to the *meta*- and *para*-positions of substituted benzenes. Large effects were found when the substituent was in the *para* position, so these results will be discussed in more detail. Much smaller effects were obtained with *meta* substituents. The addition step, upon which we focus our attention, should determine reactivity in substrate hydroxylation as the intermediate complexes were shown to rearrange easily to the final products.

In preliminary work,[63] we presented activation barriers for the face-on pathway of substrate addition to Compound I. As shown above, the side-on pathway is very similar but leads to lower barriers (by 1 to 3 kcal mol^{-1} depending on the substituent), and the corresponding transition state in the case of addition to benzene is a true saddle point, whereas the face-on "TS" is a higher order saddle-point with an additional small imaginary frequency.† For these reasons the side-on orientation was adopted in the present study for locating transition states for Compound I addition to substituted benzenes and in developing a structure–reactivity relationship. The trends in barrier heights are very similar to those obtained for the face-on TSs.

Ten different monosubstituted benzenes were modelled, with substituents ranging from strongly electron-withdrawing to electron-donating, to cover a diverse range of electronic properties. The substrates chosen in our study enable us to probe the electronic effect on the barrier heights for oxidation of a ring, which is valuable when developing a structure–activity relationship. In the protein, some of the substrates modelled here may undergo reactions other than oxidation of C–H bonds on the ring, such as hydroxylation at the aliphatic side chain. We do not therefore claim that all the compounds discussed here will undergo ring oxidation *in vivo*.[68]

The lowest route for all substrates goes through a transition state with mixed radical and electrophilic properties, comparable to those obtained in the case of unsubstituted benzene. The amount of spin and charge density on a particular substrate varies somewhat with the substituent (Table 2).

Regarding the products, the cation-like and radical-like adducts lie very close in energy for most substituted benzenes. Using a solvent continuum, even with a relatively low dielectric constant (ε = 4), predicts a stabilization of the cation-like adduct, which becomes the more favourable addition product except for strongly electron-withdrawing substituents like cyano (Table 1). This suggests that for most substrates, a pathway *via* cation-like adducts dominates in the protein environment.

The reaction barriers for the addition step are shown below (Table 3). The values obtained both with the small BSI (mainly 6-31G*) used for geometry optimisation, and with the larger BSII (6-311+G**) used in the single point computations are given for comparison; it can be seen that the results are very similar.

† Computational expense considerations prevented us from carrying out frequency calculations for all of the face-on and side-on substituted TSs.

Table 3 Reaction barriers (in kcal mol^{-1}) for addition of compound I to the *meta*- and *para*-positions of substituted benzenes

	$\Delta E^{\ddagger}$ (BSI)	$\Delta E^{\ddagger}$ (BSI, $\varepsilon = 4$)	$\Delta E^{\ddagger}$ (BSII//BSI)
p-H	16.5	21.40	15.6
p-NO_2	15.1	20.3	13.9
m-NO_2	16.0		15.8
p-Cl	15.9	21.2	15.7
m-Cl	17.1		17.0
p-NMe_2	9.9	13.5	9.4
m-NMe_2	16.6		17.3
p-OMe	13.5	18.5	12.6
m-OMe	15.9		15.4
p-CN	15.3	20.3	14.9
m-CN	16.6		16.1
p-F	15.5	20.5	15.3
m-F	17.1		16.5
p-CH_3	14.9	20.3	14.8
p-Nacetyl	13.9	18.7	14.1
p-SMe	13.3	18.6	12.8
p-NH_2	11.1	14.7	11.5

Barrier heights for substrates with substituents in the *meta* position are close to or slightly higher than in the case of unsubstituted benzene. For addition in the *para* position both strongly electron-withdrawing and electron-donating groups decrease the barrier height (Table 3). This agrees with experimental investigations by Safari *et al.*,[69] which are based on a synthetic low-molecular weight analogue of cytochrome P450 and found a similar trend in reactivity for both electron-withdrawing and electron-donating substituents.

Earlier theoretical investigations of substituent effects in aromatic hydroxylation by Jones *et al.*, using the methoxy radical as a model for Compound I,[59] also found decreased reaction barriers for compounds carrying electron-donating substituents, in agreement with our study. For electron-withdrawing substituents, however, they calculated slightly increased barriers, which might be either due to the simple model used or to the computations being performed at the lower semiempirical level.

Since the protein environment can play an important role in enzymatic reactions, a solvent continuum model was used in our calculations to approximate the effect of a polarizing medium. This raised all the barrier heights by 4–5 kcal mol^{-1} but did not affect their relative ordering (Table 3). The uniform increase in the barrier heights can be rationalised as follows: continuum solvent models make a stabilising contribution for charged, polarisable, and solvent accessible regions of a molecule. This will occur in particular for the porphyrin ring in Compound I, with its positive charge in the a_{2u} orbital. At the TS, there will be less stabilisation, as the charge on the porphyrin ring is reduced, and the steric bulk of the aromatic ring makes the iron oxide moiety and the porphyrin ring less accessible to solvent. We note that the continuum solvent computations lead to barrier heights which are perhaps slightly larger than one would expect given the known high reactivity of Compound I. However, this effect is probably not completely meaningful, as the solvent effect on the barrier height is computed relative to infinitely separated reactants, whereas the enzyme–substrate complex would be a better reference point. The most interesting observation is that the solvation model does not change the relative barrier heights much, so that the structure–activity relationship is not affected. For a more accurate description of the protein effect on reactivity, combined quantum mechanical/molecular mechanical approaches, in which the whole protein is treated atomistically, could be used.[70,71]

Oxidation of fluoroanilines and difluorobenzene

There are no experimental data available for cytochrome P450 mediated hydroxylation of substituted benzenes covering a range of substituents comparable to the ones used in our calculations. However, the influence of increasing halogen substitution on benzene and aniline hydroxylation has been investigated experimentally.[5,53] These effects are more complicated than the monosubstitution addressed above as adding another substituent to aniline or fluorobenzene can be expected to be different from the case of unsubstituted benzene. Especially for aniline, the strongly π-donating amino group will interfere with the effect of an additional halogen substituent and purely additive effects cannot necessarily be expected. Furthermore, in polysubstituted benzenes hydroxylation occurs in *para* position for one substituent but in *ortho* or *meta* position for the other substituents. In our calculations we investigated the electronic effect of fluoro substituents on the hydroxylation rate of aniline by locating transition states for oxidation of aniline itself and a series of fluoroanilines. The reaction barriers calculated for fluoro- and difluoroaniline are higher than for unsubstituted aniline, which is consistent with the experimental[5] trend of decreased reactivity upon increasing fluorination, however adding a third fluoro substituent did not lead to a further increased reaction barrier in our calculations (Table 4).

Table 4 Calculated (B3LYP/BSII//B3LYP/BSI) reaction barriers in kcal mol^{-1} for the addition of Compound I to fluorinated anilines and the natural logarithm ln k_{cat} of experimental rate constants[5]

	$\Delta E^{\ddagger}$	ln k_{cat}
Aniline	11.5	5.4
2F-Aniline	11.7	4.5
2,6F-Aniline	12.0	3.3
2,3,6F-Aniline	11.8	1.7

Table 5 Calculated (B3LYP/BSII//B3LYP/BSI) reaction barriers in kcal mol^{-1} for the addition of Compound I to 1,2-difluorobenzene in different ring positions and experimental product ratio[53]

Position	$\Delta E^{\ddagger}$	Product ratio
C3,6	16.6	0.33
C4,5	15.2	0.67

The experimental rate constants k_{cat} were obtained from an iodosobenzene-supported microsomal cytochrome P450 reaction at 25 °C.[5]

The inconsistency with experiment for the trifluoro-substituted compound might be due to slightly different enzyme kinetics or factors other than intrinsic reactivity influencing the reaction rate, *e.g.* steric or binding effects in the protein not taken into account by our small model.

As a second example we calculated the reaction barriers for two different sites of hydroxylation in 1,2-difluorobenzene. Our computations found that hydroxylation in the C4/5 position is slightly preferred over hydroxylation in the C3/6 position. The calculated difference in reaction barriers of 1.4 kcal mol^{-1} is consistent with the experimental product ratio,[53] which corresponds to a difference in barrier height of 0.4 kcal mol^{-1} (Table 5).

Structure–reactivity relationship

The experimental studies[5,53] mentioned above mainly considered the effect of halogen substituents, which only cover a small range of electronic properties. It is also difficult to draw general conclusions from substrates with multiple substituents. To analyse the effect of individual substituents, a quantitative structure reactivity relationship (QSAR) was developed from the activation barriers for monosubstituted benzenes calculated in this study. Two approaches for correlating the computed activation energies with the electronic properties of the substituents were explored: The first one uses experimentally based Hammett σ-constants as electronic parameters, the second one is based on calculated C–O bond dissociation energies of hydroxyl adducts of the substrates.

Table 6 Sigma constants for aromatic substitution in *meta*- and *para*-positions of substituted benzenes

	$\sigma_{rad\,(D)}$[a]	$\sigma_{rad\,(C)}$[b]	σ^+
H	0.09	0	0
p-NO_2	0.76	0.57	0.79
m-NO_2	—	−0.11	0.73
p-Cl	0.25	0.12	0.115
m-Cl	—	−0.04	0.40
p-NMe_2	0.61	0.9	−1.74
p-OMe	0.4	0.24	−0.78
m-OMe	—	−0.02	0.05
p-CN	0.71	0.46	0.66
m-CN	—	−0.12	0.56
p-F	0.07	−0.08	−0.075
m-F	—	−0.05	0.35
p-CH_3	0.27	0.11	−0.31
p-SMe	—	0.43	—

[a] Dinctuerck scale.[76] [b] Creary scale.[77]

Hammett substituent constants[72] have been widely used in QSAR studies to quantify the electronic effect of substituents on reaction rates.[73] There is a range of σ-scales for different reaction types. In addition to the original σ-scale, modified versions have been developed, such as σ^+ and σ^-,[74] which account for polar resonance effects in ionic reactions, and a number of radical σ-scales[75–80] $\sigma^\cdot$ to predict carbon radical stability. In an experimental investigation by Burka *et al.*[81] the overall reaction rates for the hydroxylation of monohalobenzenes by microsomal cytochromes P450 were correlated with the σ^+ Hammett constant, however only 4 substituents with very similar electronic properties were considered. Our computations cover a wide range, by including 10 different substituted benzenes. In contrast to the study by Burka,[81] the pattern of substituent effects on barriers to Compound I addition found in our calculations is indicative of radical-like behaviour. However, the computed barriers do not have a linear correlation with a purely radical Hammett σ-scale. The stabilizing effect of electron-withdrawing substituents is overestimated by the radical σ-constants while it is slightly underestimated for electron-donating substituents. Therefore, based on the dual radical and cationic nature of the transition states as computed here (Table 2), we predicted that a combination of radical and cationic σ-scales would provide a better correlation. We used a standard cationic σ-scale[74] σ^+ for electrophilic aromatic substitution, and several sets of radical σ-parameters have been tested. The best correlation‡ using a dual parameter approach was obtained with the radical σ-scale given by Creary,[78] and this is shown below (Fig. 3). It was chosen because it covered a wide range of 9 different *para* substituents and gives a good linear relation with a correlation coefficient R^2 of 0.96. In this correlation the radical parameter contributes more to describing the reactivity of a substituted benzene than the cationic parameter ($\sigma_{cat}:\sigma_{rad} = 1:2.5$).§ This is not immediately obvious from the charge and spin densities of the transition states (Table 2).

An equally good correlation was obtained using the radical σ-scale developed by Dinctuerck,[77] combined with σ_{cat}, however it included only 8 substituents. The fact that *meta* radical σ-parameters are typically very small is also in good agreement with our computations, in which the barrier heights calculated for addition in *meta* position are close to those of the unsubstituted case (Table 6).

Hammett σ-parameters are only available for a limited number of substituents due to the experimental effort involved.

‡ The parameter describing the relative importance of radical and cationic σ scales was chosen to give the best correlation. This fitting procedure was carried out manually as tests using more sophisticated multivariate methods did not yield improved results.

§ The combination of σ_{cat} and σ_{rad} used here was obtained by trial and error. More sophisticated statistical analysis led to a very similar ratio of the contributions from the two sigma scales.

Table 7 B3LYP/BSII//B3LYP/BSI relative bond dissociation energies (BDE) in kcal mol^{-1} for addition of the hydroxyl radical and cation in *meta*-and *para*-positions of substituted benzenes

	BDE_{rel} rad	BDE_{rel} cat
H	0	0
p-NO_2	2.13	−19.36
m-NO_2	−1.17	−17.45
p-Cl	0.85	0.85
m-Cl	−0.39	−6.68
p-NMe_2	3.14	40.13
m-NMe_2	−0.24	11.72
p-OMe	1.52	21.15
m-OMe	−1.15	4.20
p-CN	2.57	−13.45
m-CN	−1.16	−15.37
p-F	−0.04	0.31
m-F	−0.19	−7.83
p-CH_3	0.91	8.98
p-Nacetyl	2.09	20.11
p-SMe	2.92	20.61
p-NH_2	2.75	31.73

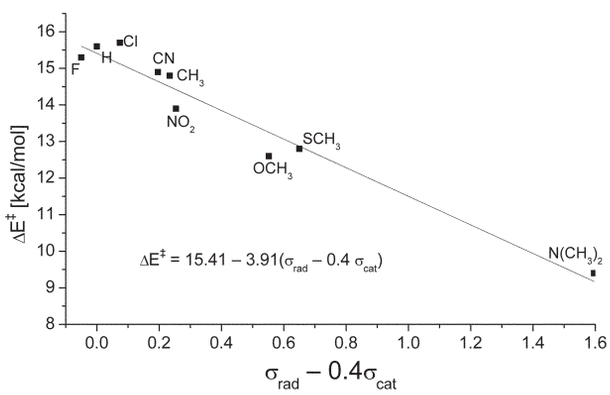

Fig. 3 Correlation of the computed reaction barriers with a combination of radical[78] and cationic[74] σ-constants.

To include substituents without σ-constants in a QSAR, calculated properties of the molecules involved, such as bond dissociation energies,[82] can provide useful alternative parameters. Thus, we developed theoretical scales for our set of substituents using bond dissociation energies that reflect the electronic properties of the individual substituents. Adducts of the substituted benzenes were formed with the OH radical and the OH cation. The C–O bond dissociation energies of the radical and cationic adducts were calculated at the same level of theory as the reaction barriers. These values relative to the bond dissociation energy of the adduct of unsubstituted benzene with the OH radical and OH cation are shown in Table 7. The C–O bond dissociation energy in this reaction is a measure of the stability of the formed benzene radicals and cations. Thus, it quantifies the influence of a particular substituent in a reaction that forms benzene cations or benzene radicals, respectively.

This theoretical scale allowed us to include NH_2 and N-acetyl as further substituents. As in the first approach using Hammett parameters, a correlation of the computed reaction barriers with a combination of the radical and the cationic relative bond dissociation energies as electronic descriptors leads to a linear relationship with a correlation coefficient R^2 of 0.82 (Fig. 4).

Again, the radical parameter has a greater weight in the correlation than the cationic one. Since bond dissociation energies for OH adducts of substituted benzenes can easily be calculated, this relationship can be extended to any substituents for which Hammett σ-constants have not been developed. This approach should be very useful for making predictions on reactivity and selectivity of drug candidates.

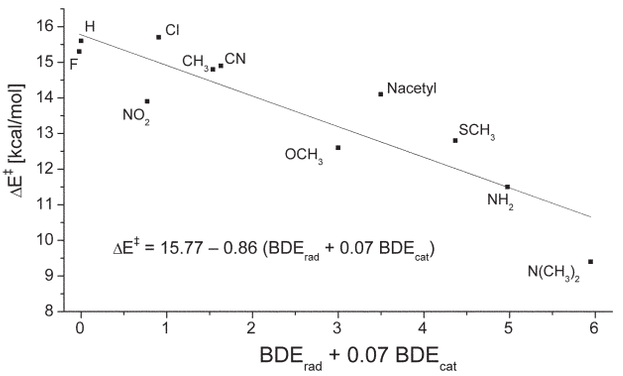

Fig. 4 Correlation of the computed reaction barriers with relative bond dissociation energies for addition of the OH radical and cation to substituted benzenes.

Conclusions

Our density functional theory study elucidates the mechanism of cytochrome P450-mediated aromatic hydroxylation and predicts the electronic effect of substituents on the intrinsic reactivity of aromatic compounds.

For these calculations a large realistic haem model of Compound I was used. Two pathways for benzene hydroxylation, differing in the orientation of approach of benzene, were explored. The electronic structure along the two pathways is very similar, but the approach with the benzene ring side-on to the porphyrin plane was found to have a lower barrier. However, the barriers along the two modes of approach are fairly similar. Depending on the substrate and the isoform of the P450 enzyme, it is therefore possible that either side-on or face-on addition could occur in enzymatic oxidation.

For the first step in the mechanism, addition of Compound I to a substrate, considerable reaction barriers for benzene and substituted benzenes (between 9.4 and 15.7 kcal mol^{-1}) were found. The comparatively low reaction barriers for subsequent rearrangements of the adducts to epoxide, ketone or phenol products suggest that the addition of Compound I is the step determining the reactivity of substrates. The lowest energy transition state shows mixed cationic and radical characteristics. Both cation-like and radical-like complexes can be formed as intermediates, however it is likely that cation-like intermediates are favoured in the protein, as they were shown to be stabilized by solvent and to rearrange rapidly to product.

Transition states for addition of Compound I to the *meta*- and *para*-positions of a range of substituted benzenes were located. Our calculations suggest that the intrinsic reactivity in arene hydroxylation is increased by both electron-withdrawing and electron-donating substituents. This is supported by an experimental study on a synthetic model of Compound I.[69] An approximation to the polarizing protein environment was made by using a solvent continuum model, which did not change the overall trend in substituent effects. However, a more realistic treatment of the protein environment by a combined quantum mechanical/molecular mechanical approach, could give further insight, as it models both steric and dielectric effects of the enzyme on the reaction.

Furthermore, the effect of multiple substituents was explored by calculating activation barriers for polyfluorinated anilines and for difluorobenzene, and the results were in qualitative agreement with experimental trends. However, factors other than intrinsic reactivity, such as steric restraints in the enzyme or different enzyme kinetics, might have to be taken into account to fully explain these reactivity trends. Also, much more intensive experimental data would be needed to check the quantitative accuracy of the calculations.

A structure–reactivity relationship was developed based on (i) the calculated activation barriers of the series of mono-substituted benzenes studied and on (ii) the knowledge of the transition state character. This shows the need for good quality electronic structure calculations to understand basic features of the mechanism. A dual-parameter approach, which employs radical and cationic σ-Hammett constants, led to a linear relation with the computed reaction barriers for Compound I addition to 8 different substituted benzenes. Additionally, a theoretical scale based on bond dissociation energies of hydroxy adducts was developed to extend the structure–reactivity relationship to substituents, for which Hammett constants are not available. Using this relationship the influence of any substituent can be predicted without the need for experimental descriptors. Being able to predict reactivity of substituted aromatics potentially helps direct the development of new drugs metabolized by the cytochromes P450.

Acknowledgements

We thank the EU (support to CMB and JNH through the MCInet TMR network), and the EPSRC (Advanced Research Fellowship to JNH), and Alessio Lodola for helpful discussions.

References

1 F. P. Guengerich, *Chem. Res. Toxicol.*, 2001, **14**, 611.
2 P. Anzenbacher and E. Anzenbacherova, *Cell. Mol. Life Sci.*, 2001, **58**, 737.
3 C. Bathelt, R. D. Schmid and J. Pleiss, *J. Mol. Model.*, 2002, **8**, 327.
4 R. E. White, M. B. McCarthy, K. D. Egeberg and S. G. Sligar, *Arch. Biochem. Biophys.*, 1984, **228**, 493.
5 N. H. Cnubben, S. Peelen, J. W. Borst, J. Vervoort, C. Veeger and I. M. C. M. Rietjens, *Chem. Res. Toxicol.*, 1994, **7**, 590.
6 M. Sono, M. P. Roach, E. D. Coulter and J. H. Dawson, *Chem. Rev.*, 1996, **96**, 2841.
7 J. T. Groves and Y. Watanabe, *J. Am. Chem. Soc.*, 1988, **110**, 8443.
8 R. Davydov, T. M. Makris, V. Kofman, D. E. Werst, S. G. Sligar and B. M. Hoffman, *J. Am. Chem. Soc.*, 2001, **123**, 1403.
9 D. G. Kellner, S. C. Hung, K. E. Weiss and S. G. Sligar, *J. Biol. Chem.*, 2002, **277**, 9641.
10 R. Rutter and L. P. Hager, *J. Biol. Chem.*, 1982, **257**, 7958.
11 R. Rutter, M. Valentine, M. P. Hendrich, L. P. Hager and P. G. Debrunner, *Biochemistry*, 1983, **22**, 4769.
12 C. M. S. A. M. Hosten, V. Palaniappan, M. M. Fitzgerald and J. Terner, *J. Biol. Chem.*, 1994, **269**, 13966.
13 J. C. Schoneboom, H. Lin, N. Reuter, W. Thiel, S. Cohen, F. Ogliaro and S. Shaik, *J. Am. Chem. Soc.*, 2002, **124**, 8142.
14 D. Harris, G. Loew and L. Waskell, *J. Inorg. Biochem.*, 2001, **83**, 309.
15 D. L. Harris and G. H. Loew, *J. Am. Chem. Soc.*, 1998, **120**, 8941.
16 G. H. Loew and D. L. Harris, *Chem Rev*, 2000, **100**, 407.
17 F. Ogliaro, S. Cohen, M. Filatov, S. P. de Visser and S. Shaik, *J. Am. Chem. Soc.*, 2000, **122**, 12892.
18 F. Ogliaro, S. Cohen, M. Filatov, D. Harris and S. Shaik, *Angew. Chem., Int. Ed.*, 2000, **39**, 3851.
19 F. Ogliaro, S. P. de Visser, J. T. Groves and S. Shaik, *Angew. Chem., Int. Ed.*, 2001, **40**, 2874.
20 S. P. de Visser, F. Ogliaro, S. Sharma and S. Shaik, *Angew. Chem., Int. Ed.*, 2002, **41**, 1947.
21 J. T. Groves and G. A. McCluskey, *J. Am. Chem. Soc.*, 1976, **98**, 859.
22 S. Kadkhodayan, E. D. Coulter, D. M. Maryniak, T. A. Bryson and J. H. Dawson, *J. Biol. Chem.*, 1995, **270**, 28042.
23 L. M. Hjelmeland, L. Aronow and J. R. Trudell, *Biochem. Biophys. Res. Commun.*, 1976, **76**, 541.
24 J. T. Groves and G. A. McClusky, *Biochem. Biophys. Res. Commun.*, 1978, **81**, 154.
25 M. H. Gelb, D. C. Heimbrook, P. Malkonen and S. G. Sligar, *Biochemistry*, 1982, **21**, 370.
26 M. Newcomb and P. H. Toy, *Acc. Chem. Res.*, 2000, **33**, 449.
27 M. Newcomb, R. Shen, Y. Lu, M. J. Coon, P. F. Hollenberg, D. A. Kopp and S. J. Lippard, *J. Am. Chem. Soc.*, 2002, **124**, 6879.
28 M. Newcomb, D. Aebisher, R. Shen, R. E. Chandrasena, P. F. Hollenberg and M. J. Coon, *J. Am. Chem. Soc.*, 2003, **125**, 6064.
29 M. Newcomb, P. F. Hollenberg and M. J. Coon, *Arch. Biochem. Biophys.*, 2003, **409**, 72.
30 T. J. Volz, D. A. Rock and J. P. Jones, *J. Am. Chem. Soc.*, 2002, **124**, 9724.

31 A. D. Vaz, D. F. McGinnity and M. J. Coon, *Proc. Natl. Acad. Sci. USA*, 1998, **95**, 3555.
32 S. Jin, T. M. Makris, T. A. Bryson, S. G. Sligar and J. H. Dawson, *J. Am. Chem. Soc.*, 2003, **125**, 3406.
33 F. Ogliaro, S. P. de Visser, S. Cohen, P. K. Sharma and S. Shaik, *J. Am. Chem. Soc.*, 2002, **124**, 2806.
34 P. K. Sharma, S. P. De Visser and S. Shaik, *J. Am. Chem. Soc.*, 2003, **125**, 8698.
35 Y. K. Kamachi T, *J. Am. Chem. Soc.*, 2003, **125**, 4652.
36 M. Hata, Y. Hirano, T. Hoshino and M. Tsuda, *J. Am. Chem. Soc.*, 2001, **123**, 6410.
37 S. Shaik, M. Filatov, D. Schroeder and H. Schwarz, *Chem. Eur. J.*, 1998, **4**, 193.
38 S. Shaik, S. P. de Visser, F. Ogliaro, H. Schwarz and D. Schroder, *Curr. Opin. Chem. Biol.*, 2002, **6**, 556.
39 N. Harris, S. Cohen, M. Filatov, F. Ogliaro and S. Shaik, *Angew. Chem., Int. Ed.*, 2000, **39**, 2003.
40 F. Ogliaro, N. Harris, S. Cohen, M. Filatov, S. P. de Visser and S. Shaik, *J. Am. Chem. Soc.*, 2000, **122**, 8977.
41 K. Yoshizawa, T. Kamachi and Y. Shiota, *J. Am. Chem. Soc.*, 2001, **123**, 9806.
42 D. Kumar, S. P. de Visser and S. Shaik, *J. Am. Chem. Soc.*, 2003, **125**, 13024.
43 D. Kumar, S. P. De Visser, P. K. Sharma, S. Cohen and S. Shaik, *J. Am. Chem. Soc.*, 2004, **126**, 1907.
44 S. P. de Visser, F. Ogliaro, P. K. Sharma and S. Shaik, *J. Am. Chem. Soc.*, 2002, **124**, 11809.
45 S. P. de Visser, F. Ogliaro and S. Shaik, *Angew. Chem., Int. Ed.*, 2001, **40**, 2871.
46 S. P. de Visser, F. Ogliaro, N. Harris and S. Shaik, *J. Am. Chem. Soc.*, 2001, **123**, 3037.
47 D. Kumar, S. P. De Visser and S. Shaik, *J. Am. Chem. Soc.*, 2004, **126**, 5072.
48 D. M. Jerina, J. W. Daly, B. Witkop, P. Zaltzman-Nirenberg and S. Udenfriend, *J. Am. Chem. Soc.*, 1968, **90**, 6525.
49 D. M. Jerina and J. W. Daly, *Science*, 1974, **185**, 573.
50 G. Guroff, J. W. Daly, D. M. Jerina, J. Renson, B. Witkop and S. Udenfriend, *Science*, 1967, **157**, 1524.
51 J. Koerts, A. E. Soffers, J. Vervoort, A. De Jager and I. M. C. M. Rietjens, *Chem. Res. Toxicol.*, 1998, **11**, 503.
52 K. R. Korzekwa, D. C. Swinney and W. F. Trager, *Biochemistry*, 1989, **28**, 9019.
53 I. M. C. M. Rietjens, A. E. Soffers, C. Veeger and J. Vervoort, *Biochemistry*, 1993, **32**, 4801.
54 O. Zakharieva, M. Grodzicki, A. X. Trautwein, C. Veeger and I. M. C. M. Rietjens, *J. Biol. Inorg. Chem.*, 1996, **1**, 192.
55 O. Zakharieva, M. Grodzicki, A. X. Trautwein, C. Veeger and I. M. C. M. Rietjens, *Biophys. Chem.*, 1998, **73**, 189.
56 S. Shaik and P. S. de Visser, *J. Am. Chem. Soc.*, 2003, **125**, 7413.
57 A. E. M. F. Soffers, M. G. Boersma, W. H. J. Vaes, J. Vervoort, B. Tyrakowska, J. L. M. Hermens and I. M. C. M. Rietjens, *Toxicol. in Vitro*, 2001, **15**, 539.
58 L. Ridder, A. J. Mulholland, I. M. C. M. Rietjens and J. Vervoort, *J. Am. Chem. Soc.*, 2000, **122**, 8728.
59 J. P. Jones, M. Mysinger and K. R. Korzekwa, *Drug Metab. Dispos.*, 2002, **30**, 7.
60 J. N. Harvey, *J. Am. Chem. Soc.*, 2000, **122**, 12401.
61 P. E. Siegbahn and M. R. Blomberg, *Chem. Rev.*, 2000, **100**, 421.
62 P. E. Siegbahn, *Q. Rev. Biophys.*, 2003, **36**, 91.
63 C. M. Bathelt, L. Ridder, A. J. Mulholland and J. N. Harvey, *J. Am. Chem. Soc.*, 2003, **125**, 15004.
64 Jaguar 4.2, Schrodinger, Inc., Portland, OR, 1991–2002.
65 J. P. Hay and W. R. Wadt, *J. Chem. Phys.*, 1985, **82**, 299.
66 M. J. Frisch, G. W. Trucks, H. B. Schlegel, G. E. Scuseria, M. A. Robb, J. R. Cheeseman, V. G. Zakrzewski, J. A. Montgomery, R. E. Stratmann, J. C. Burant, S. Dapprich, J. M. Millam, A. D. Daniels, K. N. Kudin, M. C. Strain, O. Farkas, J. Tomasi, V. Barone, M. Cossi, R. Cammi, B. Mennucci, C. Pomelli, C. Adamo, S. Clifford, J. Ochterski, G. A. Petersson, P. Y. Ayala, Q. Cui, K. Morokuma, D. K. Malick, A. D. Rabuck, K. Raghavachari, J. B. Foresman, J. Ciolowski, J. V. Ortiz, B. B. Stefanov, G. Liu, A. Liashenko, P. Piskorz, I. Komaromi, R. Gomperts, R. L. Martin, J. Fox, T. Keith, M. A. Al-Laham, C. Y. Peng, A. Nanayakkara, C. Gonzalez, M. Head-Gordon, E. S. Replogle, J. A. Pople, *GAUSSIAN98*, Gaussian, Inc., Pittsburgh, PA, 1998.
67 K. Korzekwa, W. Trager, M. Gouterman, D. Spangler and G. H. Loew, *J. Am. Chem. Soc.*, 1985, **107**, 4273.
68 However, we point out that benzene is indeed metabolised by cytochrome P450 2E1 in the human liver; M. J. Seaton, P. M. Schlosser, J. A. Bond and M. A. Medinsky, *Carcinogenesis*, 1994, **15**, 1799.
69 N. Safari, F. Bahadoran, M. R. Hoseinzadeh and R. Ghiasi, *J. Porphyrins Phthalocyanines*, 2000, **4**, 285.
70 L. Ridder and A. J. Mulholland, *Curr. Top. Med. Chem.*, 2003, **3**, 1241.
71 J. C. Schoneboom, S. Cohen, H. Lin, S. Shaik and W. Thiel, *J. Am. Chem. Soc.*, 2004, **126**, 4017.
72 C. Hansch, A. Leo and R. W. Taft, *Chem. Rev.*, 1991, **91**, 165.
73 C. Hansch and H. Gao, *Chem. Rev.*, 1997, **97**, 2995.
74 R. Tayler, *Electrophilic aromatic substitution*, Wiley, Chichester, 1990.
75 L. Liu, Y. H. Cheng, Y. Fu, R. Chen and Q. X. Guo, *J. Chem. Inf. Comput. Sci.*, 2002, **42**, 1164.
76 X.-K. Jiang, *Acc. Chem. Res.*, 1997, **30**, 283.
77 S. Dinctuerk and R. A. Jackson, *J. Chem. Soc., Perkin Trans. 2*, 1981, 1127.
78 X. Creary, M. E. Mehrsheikh-Mohammadi and S. McDonald, *J. Org. Chem.*, 1987, **52**, 3254.
79 T. H. Fisher, S. M. Dershem and M. L. Prewitt, *J. Org. Chem.*, 1990, **55**, 1040.
80 J. M. Dust and D. R. Arnold, *J. Am. Chem. Soc.*, 1983, **105**, 1221.
81 L. T. Burka, T. M. Plucinski and T. L. Macdonald, *Proc. Natl. Acad. Sci. USA*, 1983, **80**, 6680.
82 Y. D. Wu, C. L. Wong, K. W. Chan, G. Z. Ji and X. K. Jiang, *J. Org. Chem.*, 1996, **61**, 746.